

Titanium–oxo–Clusters with Dicarboxylates: Single-Crystal Structure and Photochromic Effect

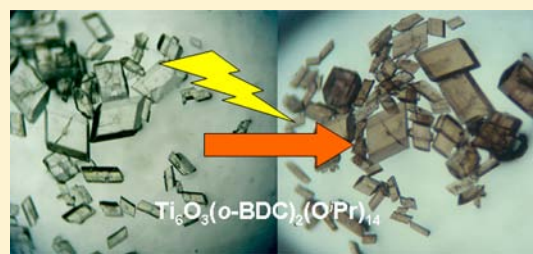
Yin-Yin Wu,[†] Wen Luo,[†] Yu-Hong Wang,[†] Ya-Yang Pu,[†] Xiang Zhang,[†] Li-Sheng You,[†] Qin-Yu Zhu,^{*,†,‡} and Jie Dai^{*,†,‡}

[†]Department of Chemistry & Key Laboratory of Organic Synthesis of Jiangsu Province, Soochow University, Suzhou 215123, People's Republic of China

[‡]State Key Laboratory of Coordination Chemistry, Nanjing University, Nanjing 210093, People's Republic of China

Supporting Information

ABSTRACT: Two titanium-oxo-clusters $\text{Ti}_6\text{O}_4(\text{o-BDC})_2(\text{o-BDC}^i\text{Pr})_2(\text{O}^i\text{Pr})_{10}$ (**1**) and $\text{Ti}_6\text{O}_3(\text{o-BDC})_2(\text{O}^i\text{Pr})_{14}$ (**2**) (BDC = benzene dicarboxylate) were prepared by one-step in situ solvothermal synthesis. The compounds are the rare examples of the dicarboxylate-substituted titanium-oxo-clusters. Their crystal structures are successfully measured by single-crystal X-ray analysis. The Ti_6 oxo-clusters of **1** and **2** are constructed by two dual corner-missing cube subunit, Ti_3O_3 . The two subunits are linked by double μ_3 -O bridges for **1** and single μ_2 -O bridge for **2**, respectively, and the latter is a new type of carboxylate substituted titanium-oxo-cluster. A photochromic effect was observed upon irradiation of the crystals in the presence of alcohol. The light irradiation changed the color of the crystals from transparent to purple-gray. The Ti(III) signal was detected after the irradiation, and when the sample was exposed in air, superoxide diatomic $\text{O}_2^{\bullet-}$ radical was found. Photodegradation of the methyl orange in aqueous dispersions of microcrystals of the cluster **2** was carried out under UV cut white light with the assistance of H_2O_2 .



INTRODUCTION

Nanostructural titanium dioxide has been widely used as a photocatalyst for solar energy conversion and environmental applications, because of its low toxicity, abundance, high photostability, and high efficiency.¹ The titanium oxo-clusters, as the model of the bulk nanoscale titanium oxides, offer the opportunity to understand the information of the bulk nanoscale oxides in terms of both atomic structure and chemical reactivity.^{2,3} The titanium-oxo-clusters $[\text{Ti}_n\text{O}_m(\text{OR})_x(\text{L})_y]$ exhibit rich variations in structural types characterized by the different coordination modes of the ligands (O, OR, and L), in linkages of the coordination polyhedra, in degrees of condensation O/Ti, and in coordination numbers of titanium atoms, which have been reviewed recently by Rozes.⁴

The carboxylate-substituted titanium oxo-clusters constitute an important subclass of titanium-oxo-clusters whose nuclearity varies from 2, $[\text{Ti}_2\text{O}(\text{O}^i\text{Pr})_2(\text{HO}^i\text{Pr})_2(\text{OOC}\text{CCl}_3)_4]$,⁵ to 28, $[\text{Ti}_{28}\text{O}_{40}(\text{O}^i\text{Bu})_{20}(\text{OOAc})_{12}]$.³ The hydrolytic stability of the carboxylate-coordinated titanium oxo-alkoxy clusters is higher than that of the pure titanium oxo-alkoxy clusters. About 20 monocarboxylates have been used for the synthesis of the carboxylate-coordinated titanium-oxo clusters $[\text{Ti}_n\text{O}_m(\text{OR})_x(\text{OOCR}')_y]$, but no crystal structure with dicarboxylate has been reported for such clusters, except $\text{Ti}_8\text{O}_8(\text{OH})_4(\text{O}_2\text{C}-\text{C}_6\text{H}_4-\text{CO}_2)_6$, which is a recently reported titanium-oxo-hydroxy cluster with dicarboxylate linkers.⁶ However, only microcrystalline sample of the compound was obtained, and the crystal structure was solved by ab initio on

the sample using powder X-ray diffraction (XRD) data by a direct method.

We successfully introduced phthalic acid (benzene dicarboxylate acid, H_2BDC) into titanium-oxo clusters and got two new compounds, $\text{Ti}_6\text{O}_4(\text{o-BDC})_2(\text{o-BDC}^i\text{Pr})_2(\text{O}^i\text{Pr})_{10}$ (**1**) and $\text{Ti}_6\text{O}_3(\text{o-BDC})_2(\text{O}^i\text{Pr})_{14}$ (**2**), in large single crystals, by one step in situ solvothermal synthesis. Crystal structures of such dicarboxylate clusters are first obtained by single-crystal analysis. Moreover, the crystals showed a reversible photochromic behavior in the presence of alcohol, and Ti(III) signal was detected after irradiation. In the presence of oxygen, back-oxidation of titanium(III) ions into titanium(IV) can be associated with the reduction of molecular oxygen into superoxide diatomic $\text{O}_2^{\bullet-}$ radical. Photodegradation of the Methyl Orange with the assistance of tiny amount of H_2O_2 in aqueous dispersions of microcrystals of the cluster **2** is investigated.

EXPERIMENTAL SECTION

General Remarks. All analytically pure reagents are purchased commercially and used without further purification. The IR spectra are recorded as KBr pellets on a Nicolet Magna 550 FT-IR spectrometer. Elemental analyses of C and H are performed using a VARIDEL III elemental analyzer, while the Ti contents are determined by titration using $\text{Al-NH}_4\text{Fe}(\text{SO}_4)_2$

Received: May 24, 2012

Published: August 7, 2012

method. Solid-state room-temperature optical diffuse reflectance spectra of the microcrystal samples are obtained with a Shimadzu Model UV-3150 spectrometer. Room-temperature XRD data are collected on a D/MAX-3C diffractometer using a Cu tube source (Cu K α , $\lambda = 1.5406 \text{ \AA}$). Solid-state ESR spectra are recorded by an EMX-10/12 spectrometer at 110 K. Thermal analysis is conducted on a TGA-DCS 6300 micro-analyzer. The samples are heated under a nitrogen stream of 100 mL min⁻¹ with a heating rate of 20 °C min⁻¹.

Synthesis of Ti₆O₄(*o*-BDC)₂(*o*-BDC-*Pr*)₂(*O*^{*i*}Pr)₁₀ (1). Analytically pure Ti(*O*^{*i*}Pr)₄ (0.1 mL, 0.26 mmol) and phthalic acid (0.03 g, 0.18 mmol) are mixed in 0.5 mL anhydrous toluene. The mixture is placed in a thick Pyrex tube (0.7 cm diameter, 18 cm length) and quickly degassed by argon. The sealed tube is heated under autogenous pressure at 100 °C for 6 days to yield colorless rhombous crystals (32% yield based on Ti(*O*^{*i*}Pr)₄). The crystals are rinsed with toluene, and dried. The compound is preserved under dark and dry environment. Anal. Calcd for C₆₈H₁₀₀O₃₀Ti₆ (MW 1684.88): C, 48.48; H, 5.98; Ti, 17.05. Found: C, 47.90; H, 5.63; Ti, 17.63. Important IR data (KBr, cm⁻¹): 2970(s), 2930(m), 1736(s), 1568(s), 1475(s), 1271(m), 1130(vs), 1007(s), 947(w), 854(m), 563(s), 511(m).

Synthesis of Ti₆O₃(*o*-BDC)₂(*O*^{*i*}Pr)₁₄ (2). Analytically pure Ti(*O*^{*i*}Pr)₄ (0.1 mL, 0.26 mmol), and phthalic acid (0.03 g, 0.18 mmol) are mixed in 0.5 mL of anhydrous isopropanol. The mixture is placed in a thick Pyrex tube (0.7 cm diameter, 18 cm length) and quickly degassed by argon. The sealed tube is heated under autogenous pressure at ~100 °C for 6 days to yield colorless hexagonal prism crystals (40% yield based on Ti(*O*^{*i*}Pr)₄). The crystals are rinsed with isopropanol, and dried. The compound is stable and preserved under dark and dry environment. Anal. Calcd for C₅₈H₁₀₆O₂₅Ti₆ (MW 1490.74): C, 46.73; H, 7.17; Ti, 19.27. Found: C, 46.48; H, 7.36; Ti, 20.01. Important IR data (KBr, cm⁻¹): 2970(m), 2930(w), 2862(w), 1525(m), 1489(w), 1413(vs), 1121(m), 1012(s), 952(m), 855(w), 593(m), 486(w).

X-ray Crystallographic Study. The measurement is carried out on a Rigaku Mercury CCD diffractometer at low temperature with graphite-monochromated Mo K α ($\lambda = 0.71075 \text{ \AA}$) radiation at 223 and 192 K. X-ray crystallographic data for all the compounds are collected and processed using CrystalClear (Rigaku).⁷ The structures are solved by direct methods using SHELXS-97 and the SHELXS-97 program, and the refinement is performed against F^2 using SHELXL-97.⁸ All the non-hydrogen atoms are refined anisotropically. The hydrogen atoms are positioned with idealized geometry and refined with fixed isotropic displacement parameters. Relevant crystal data, collection parameters, and refinement results can be found in Table 1.

Photochemical Degradation of Dye. A 70-W halogen lamp, positioned 15 cm over the surface of the reaction solution, is employed as light source. A UV cutoff filter (Kenko) is used to eliminate radiation at wavelengths below 420 nm and to ensure illumination by visible light only. The aqueous dispersions of catalysts are prepared by addition of 22 mg **2** to 30 mL aqueous solutions containing the dye of Methyl Orange (MO). Prior to irradiation, the suspensions are magnetically stirred in the dark for ca. 1.0 h to ensure the establishment of adsorption/desorption equilibrium of dye on the surface of the microcrystals. The dispersions are added H₂O₂ (3%, 150 μ L) before irradiation. At given time intervals, 2 mL of aliquots are sampled, centrifuged, and then the supernate are analyzed by recording variations of the absorption spectra.

Table 1. Crystal Data and Structural Refinement Parameters for 1 and 2

	1	2
formula	C ₆₈ H ₁₀₀ O ₃₀ Ti ₆	C ₁₇₄ H ₃₁₈ O ₇₅ Ti ₁₈
Fw	1684.88	4471.91
cryst size (mm ³)	0.40 × 0.38 × 0.25	0.50 × 0.50 × 0.30
cryst syst	triclinic	monoclinic
space group	$P\bar{1}$	$P2_1/n$
<i>a</i> (Å)	10.9658(12)	171044(10)
<i>b</i> (Å)	13.3174(14)	39.111(2)
<i>c</i> (Å)	15.1216(15)	34.202(2)
α (deg)	95.939(2)	90.00
β (deg)	102.390(2)	90.244(2)
γ (deg)	107.205(2)	90.00
<i>V</i> (Å ³)	2027.1(4)	22880(2)
<i>Z</i>	1	4
ρ_{calcd} (g cm ⁻³)	1.380	1.298
<i>F</i> (000)	880	9432
μ (mm ⁻¹)	0.640	0.666
<i>T</i> (K)	223(2)	193(2)
<i>R</i> _{int}	0.0335	0.0735
reflns collected	19526	106645
unique reflns	9131	40004
observed reflns	7303	28578
no. params	482	2486
restraints	30	10
GOF on F^2	1.010	1.123
$R_1[I > 2\sigma(I)]/R_1^a$	0.0603/0.0792	0.0892/0.1272
$wR_2[I > 2\sigma(I)]/wR_2^b$	0.1581/0.1743	0.1329/0.1503

$$^a R_1 = \sum |F_o| - |F_c| / \sum |F_o|, \quad ^b wR_2 = \{[\sum (w(F_o^2 - F_c^2)^2) / \sum (w(F_o^2)^2)]^{1/2}\}.$$

RESULTS AND DISCUSSION

Synthesis. Compounds **1** and **2** are obtained as colorless crystals by a similar solvothermal technique. The experimental conditions are optimized in order to obtain single crystals with high quality. By carefully selecting the mole ratio and the volume of the solvents, bulky crystals of the clusters crystallize directly from the reaction mixtures after a few days. Most carboxylate-substituted titanium(IV)-oxo- clusters were obtained by mixing Ti(OR)₄ and the corresponding acid, and the solutions were refluxed or solvothermal treated, but usually the excessive solvent must be removed slowly under inert atmosphere for the crystallization. Only a few examples were reported that the single crystals could be obtained directly from the solvothermal systems: [Ti₄O(OEt)₁₅(ZnCl)] (from ref 9) and [Ti₂₈O₄₀(*O*^{*t*}Bu)₂₀(OAc)₁₂] (from ref 3). The in situ crystal growth using titanium(IV) isopropoxide, [Ti(*O*^{*i*}Pr)₄], is better than that using titanium(IV) *n*-butyloxide, [Ti(*O*^{*n*}Bu)₄], in this case, due to the high hydrolysis tendency of [Ti(*O*^{*i*}Pr)₄]. The production of water allows a controllable growth of carboxylate-substituted oxo clusters by hydrolysis of OR groups. Temperature has an important role in the preparation of the compounds and should not be too high. No crystals—only clear liquid—are obtained when the temperature is higher than 100 °C or the reaction time is prolonged.

In a general way, ester was observed by the reaction of Ti(OR)₄ with more than one molar equivalent of carboxylic acid.⁴ For a dicarboxylic acid, using more than half one molar equivalent of the acid in the reaction results in the formation of carboxylate ester, a product of competing reactions. The fundamental reactions of Ti(OR)₄ with Ph(COOH)₂ (BCD) can be found in the Supporting Information. Compound **1** is a

good example of reaction system, in which carboxylate ester is characterized crystallographically (see the structural section). To further characterize the bulk samples of **1** and **2**, IR, XRD, TGA, and optical diffuse-reflection spectrum are carried out. The XRD patterns of the powder microcrystals are in agreement with that simulated from the data of single-crystal analysis (see Figure S1 in the Supporting Information). For each compound, the FTIR stretches of the BDC acid (1568 and 1432 cm^{-1} for **1**, and 1556 and 1413 cm^{-1} for **2**) indicate the chelating coordination of the carboxyl group. Isopropoxy groups are detected by the $\nu_{\text{C-H}}$ (between 2970 cm^{-1} and 2850 cm^{-1}) and $\nu_{\text{Ti-O-C}}$ (1013 cm^{-1} and 1007 cm^{-1}) vibrations. The bands below 720 cm^{-1} are attributed to the Ti–O vibrations (see Figure S2 in the Supporting Information). The bands at 1735 and 1271 cm^{-1} for **1** are assigned to the C=O and C–O–C characteristic bands of the ester group of *o*-BDC-*i*Pr that is absent in the spectrum of **2**. The TGA results are also given in the Supporting Information (Figure S3).

Structures of Compounds 1 and 2. The ball–stick plots of the cores of **1** and **2** are shown in Figure 1 (the isopropane

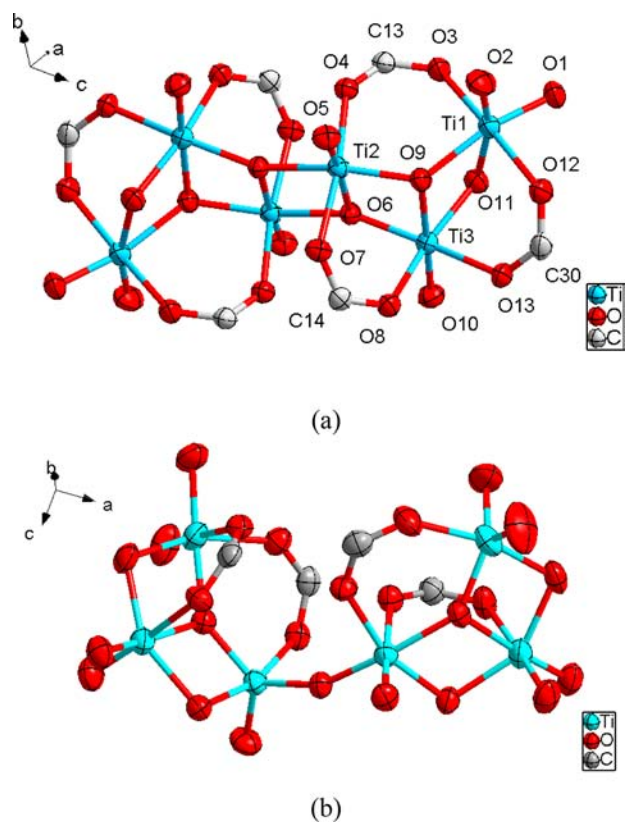


Figure 1. The core structures of compounds (a) **1** and (b) **2** with 50% thermal ellipsoid; the isopropane and benzene groups are omitted for the sake of clarity.

and benzene groups are omitted for clarity). The structures of this family of compounds are best described as two trinuclear oxo- Ti_3 subunits linked by $\mu_3\text{-O}$ or $\mu_2\text{-O}$ bridges. The two Ti_3O_3 clusters are linked by two $\mu_3\text{-O}$ bridges in **1** and by one $\mu_2\text{-O}$ bridge in **2**, forming Ti_6 clusters. The O6-Ti2 , O6-Ti3 , and $\text{O6-Ti}\#$ ($\#$: $1-x, -y, 1-z$) distances of $\mu_3\text{-O}$ bridges in **1** are $2.080(2)$, $1.872(2)$, and $1.958(2)\text{ \AA}$, and the O11-Ti2 and O11-Ti4 distances of $\mu_2\text{-O}$ bridges in **2** are $1.784(3)$ and

$1.847(3)\text{ \AA}$, shorter than the former. The Ti–O distances of the $\mu_3\text{-O}$ bridges at the Ti_3O_3 clusters in **1** and **2** are comparable to each other. The remainder sites of the structures are compensated by *O*^{*i*}Pr and carboxylate groups. Important Ti–O bond lengths and angles are listed in Tables S1 and S2 in the Supporting Information). Besides the difference in central $\mu\text{-O}$ bridges, the coordination number of the titanium(IV) in compound **1** is also different from that in **2**. Figure 2 illustrates

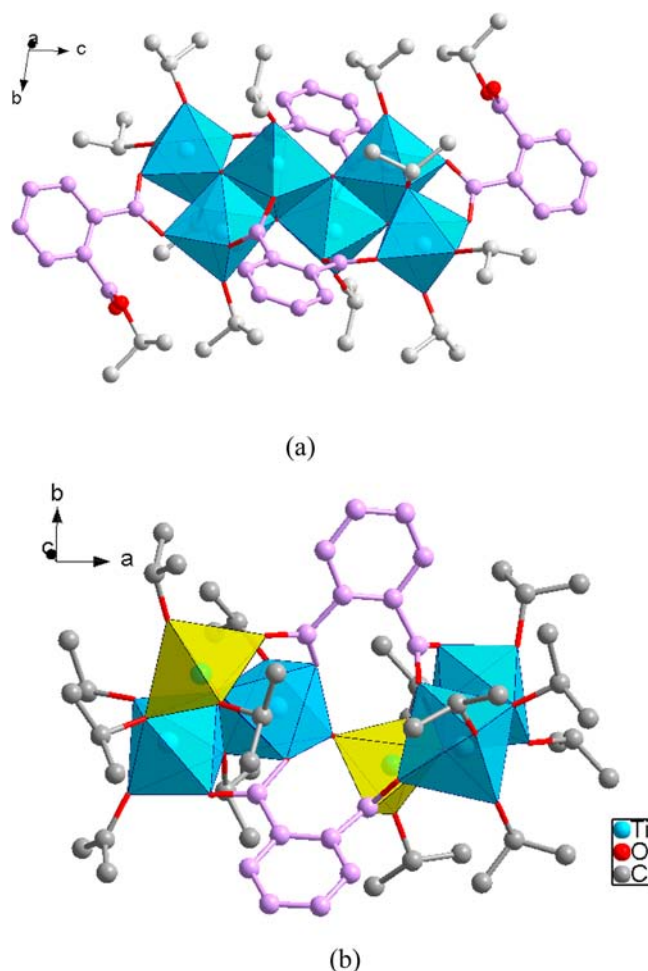


Figure 2. Clusters of (a) **1** and (b) **2**, illustrating the coordination polyhedra of each Ti and the coordination of BDC.

the coordination polyhedra of each Ti in **1** and **2** and the coordination of BDC. The coordination spheres of six Ti are all octahedral in **1**, but four octahedral and two bipyramidal in **2**. All the *o*-BDC are in bridging modes that two of the carboxylate groups coordinate to different Ti_3 subunits, while two mono-esterified *o*-BDC in **1** only act as monocarboxylate coordinating at two sides of the Ti_6 cluster. All the bridging modes of the *o*-BDC in **1** and **2** are asymmetrical. As an example, in compound **1**, one carboxylate group bridges Ti1 and Ti3 , and the other bridges Ti1 and Ti2 of the Ti_3O_3 subcluster (Figure 3).

The skeletal arrangements of known Ti_6 carboxylate substituted oxo-clusters are shown in Figures 4a–c, except the hexaprism of $[\text{Ti}_6\text{O}_6(\text{OR})_6(\text{OOCR}')_6]^{5,10}$. The basic structural arrangements of this family of compounds are best described as two trinuclear oxo-centered units, $[\text{TiO}]_4$ cubes with one or two corners removed, linked by oxo-bridge with a

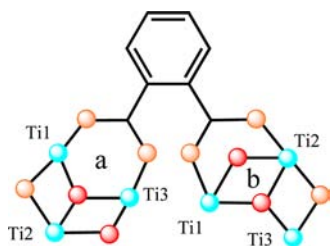


Figure 3. Asymmetric bridging mode of *o*-BDC in **1** and **2**.

center of symmetry.^{4,11} The skeletal arrangements of the two new Ti_6 carboxylate substituted oxo-clusters are shown in Figures 4d and 4e. Similar to the type (c) compound (Figure 4c), there are two dual corner-missing cube subunits Ti_3O_3 bridged by two μ_3-O in compound **1** (Figure 4d), but with different arrangement. The skeletal arrangement of **2** is a new type of Ti_6 carboxylate substituted oxo-clusters that has only a mono μ_2-O bridge in cluster center (Figure 4e).

Studies of the Photochromic Effect. A photochromic effect is observed on both **1** and **2** upon UV–vis excitation by a halogen lamp or sunlight in the presence of alcohol. The light irradiation changes the color of the crystals from transparent to purple-gray (see Figure 5 and Figure S4 in the Supporting Information). Optical diffuse reflectance spectra of the micro crystal samples of **2** before and after irradiation are measured and the absorption data in the visible-near-IR range are calculated from the reflectance using the Kubelka–Munk function, $\alpha/S = (1 - R)^2/(2R)$ (from ref 12; see Figure 6). The colored photochromic sample exhibits a new broad band with a maximum located at 2.46 eV (504 nm), and it can be assigned to the overlapped Ti(III) d–d transition and intervalence transition. The ESR spectra recorded at 110 K for the samples of **1** and **2** after irradiation are shown in Figure 7. The irradiated samples exhibit characterized signals of paramagnetic Ti(III) centers in a distorted rhombic ligand field with parameters 1.968 (g_1), 1.943 (g_2), 1.923 (g_3), and 1.970 (g_1), 1.944 (g_2), 1.926 (g_3), respectively.⁶ To ensure the Ti(III) ions were not oxidized in the sample preparation, the crystal samples for ESR measurement were not powdered. For this reason, the signals show some noise. Moreover, when the gray

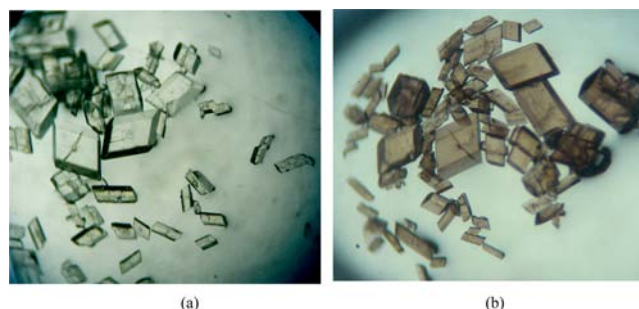


Figure 5. Light irradiation changes the color of the crystals of **1** from (a) transparent to (b) purple-gray.

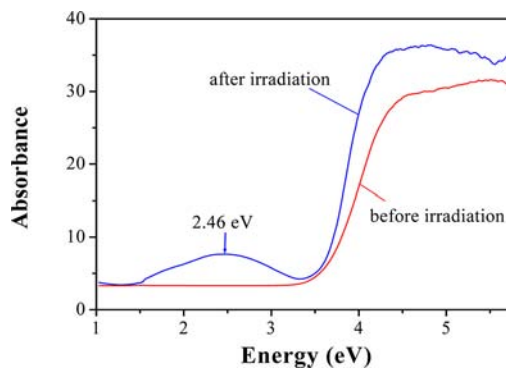


Figure 6. Absorption spectra of compound **2**, showing the characteristic photoinduced change.

samples are ground in air for a short time (several minutes), super oxide diatomic $O_2^{\bullet-}$ ion is detected with the disappearing of Ti(III) signal. The observed $O_2^{\bullet-}$ resonances of **1** and **2** are 2.029 (g_1), 2.013 (g_2), 2.007 (g_3), and 2.030 (g_1), 2.013 (g_2), 2.008 (g_3), respectively, which disappear gradually by laying the gray sample in air and avoid the light irradiation (see Figure 8 and Figure S5 in the Supporting Information). It is also demonstrated by the color change from gray to pale yellow. The ESR result is similar to the characteristic orthorhombic signals reported for super oxide diatomic $O_2^{\bullet-}$ ions.¹³

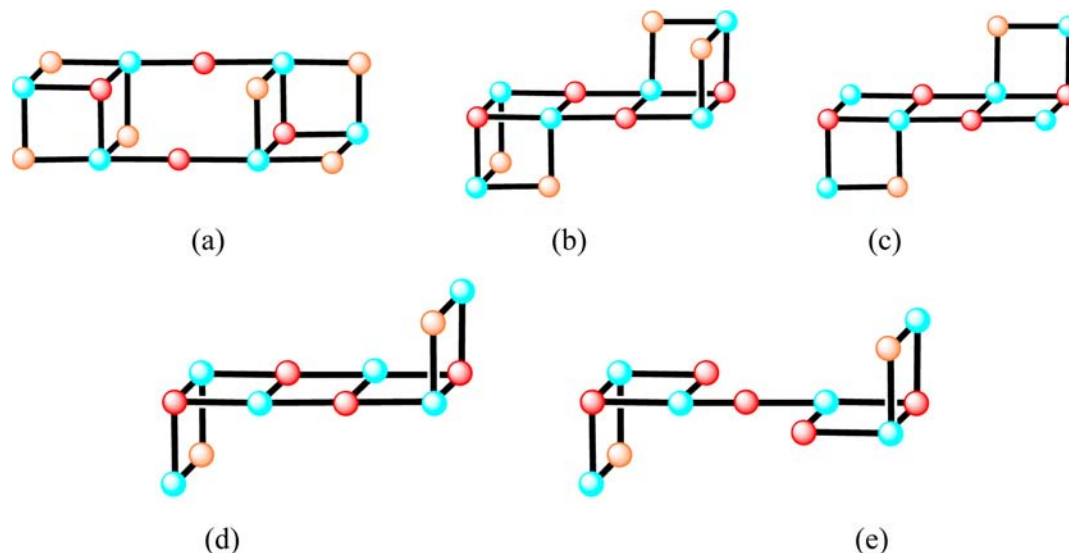


Figure 4. Skeletal arrangements of the Ti_6 carboxylate-substituted oxo clusters: (a–c) reported, (d) **1**, and (e) **2**.

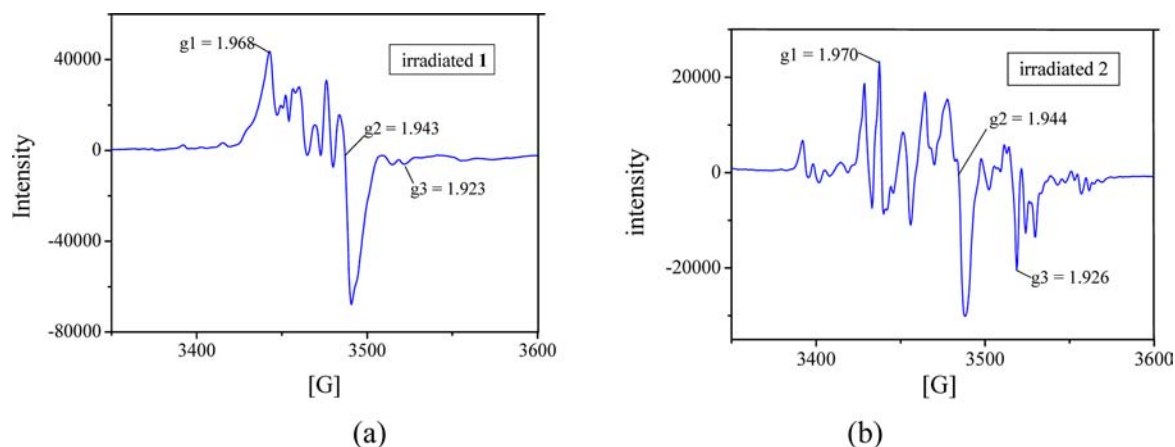


Figure 7. ESR spectra recorded at 110 K for the gray samples (after irradiation) of (a) 1 and (b) 2.

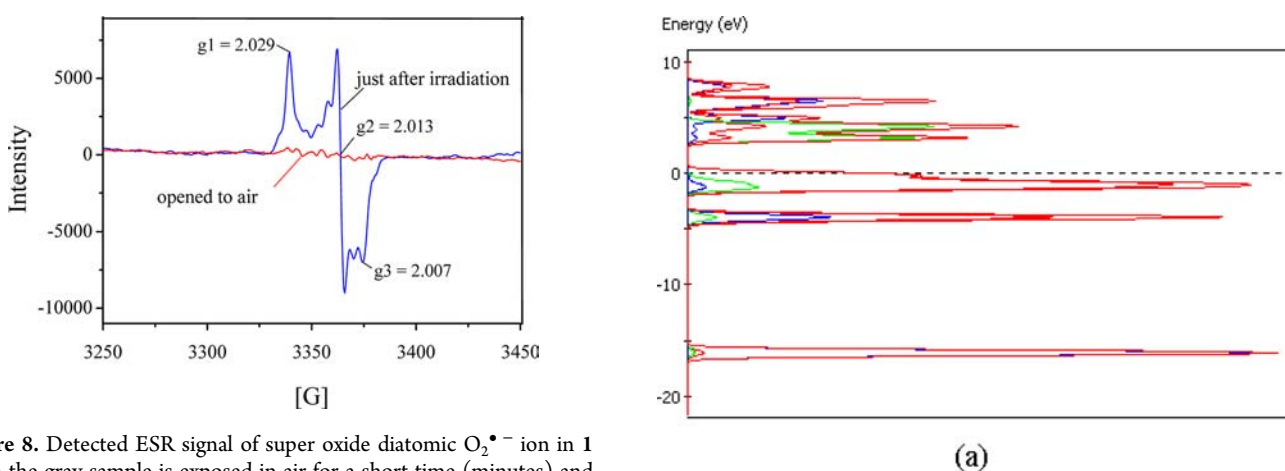


Figure 8. Detected ESR signal of super oxide diatomic $\text{O}_2^{\bullet-}$ ion in 1 when the gray sample is exposed in air for a short time (minutes) and long time (1 day).

The experiments reveal that the cluster structures play an important role in the photochromic effect, because no such phenomenon happens if $\text{Ti}(\text{O}^i\text{Pr})_4$ is used under the same condition. The density of states (DOS) of the simplified models of $\text{Ti}(\text{OH})_4$ and trinuclear $\text{Ti}_3\text{O}(\text{OH})_7$ are calculated by Material Studio program (Release 4.0; Accelrys Software, Inc., San Diego, 2006). The result is shown in Figure 9. It is seen clearly from the DOS plots that the energy of unoccupied Ti 3d orbit (green) of the $\text{Ti}(\text{OH})_4$ is $\sim 2.5\text{--}5.0$ eV, while that of the $\text{Ti}_3\text{O}(\text{OH})_7$ is approximately $-1.0\text{--}3.0$ eV. The dropped band energy considerably stabilized the Ti(III) species and the broadened band structure (trinuclear) is in favor of electron conjugation.

Single-crystal structure analysis of the irradiated gray crystal of 1 is performed to know if the crystal parameters, such as bond distances and angles, are changed due to the reduction of Ti(IV) to Ti(III). The result is negative that no obvious changes are detected, which indicate that the photochemical reaction only occurs on the surface of the crystals. Therefore, it further demonstrates that alcohol as a reduction reagent is necessary in the photoassisted reduction of Ti(IV) into Ti(III). It has been said that such reaction is of interest because it underlines a possible photocatalytic activity for titanium-oxoclusters.

Photochemical Degradation of Methyl Orange. During the past decades, photocatalytic processes involving TiO_2 semiconductor particles under illumination have been shown

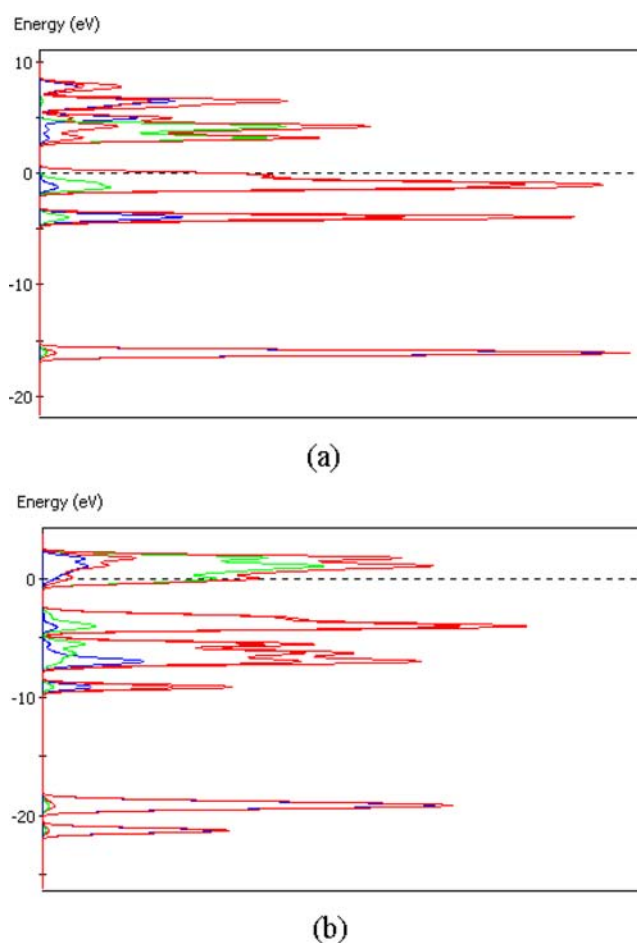


Figure 9. Density of states (DOS) plots of the simplified models of (a) $\text{Ti}(\text{OH})_4$ and (b) $\text{Ti}_3\text{O}(\text{OH})_7$; the red, blue, green, and red contour lines are the s, p, d, and total DOS plots, respectively.

to be advantageous and useful in the photodegradation of dyes.¹⁴ The photoinduced $\text{O}_2^{\bullet-}$ ions can be correlated with the photocatalytic effect. The photodegradation of the Methyl Orange (MO) in aqueous dispersions of microcrystals of the cluster 2 are carried out under UV cut white light (>420 nm) in the presence of a tiny amount of H_2O_2 .¹⁵ The degradation of MO is investigated under various conditions, including the use of irradiation or in darkness, and with or without H_2O_2 . It is interesting that a synergistic effect is observed in the system of

TiO₂/H₂O₂ for the photodegradation of MO. The reaction is not obvious if no H₂O₂ is added. As shown in Figure 10, it is

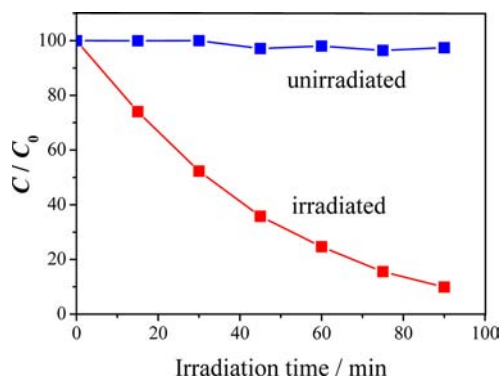


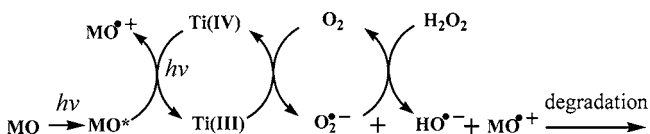
Figure 10. Photodegradation of MO versus irradiation time: blank (blue) and illuminated by visible irradiation (red) in a 30-mL aqueous solution of MO (0.10 mmol/L) with 22 mg of suspended **2** and a catalytic amount of H₂O₂ (3%, 150 μL).

noted that more than 90% decay of MO is observed during 100 min in the system of TiO-cluster/H₂O₂ under the irradiation of visible light. However, no obvious decay of MO is observed in the same system without the irradiation (in darkness). The concentration of MO (C/C_0) decreases exponentially with irradiation time via a pseudo-first-order process ($k = 0.0258(8) \text{ min}^{-1}$, $R = 99.7\%$; see Figure S6 in the Supporting Information).

The photodegradation of dyes in aqueous dispersions of TiO₂ have been studied in some detail. The major steps in the mechanism under visible irradiation have been summarized.¹⁵ The synergistic effect of H₂O₂ may be rationalized by the following:

- (1) The interaction between H₂O₂ and TiO cluster leads to the formation of titanium peroxide complex and various radical anions that act as oxidizing species with the assistance of visible light.
- (2) The hydrogen peroxide reacts with O₂^{•-}, leading to the active OH^{•-}, which is responsible for the degradation of dyes.^{15,16}

Considering the visible-light-induced and dye-sensitized reaction, and the evidence of Ti(IV)/Ti(III) transfer and the detected O₂^{•-}, the mechanism of the reaction is suggested as follows:



CONCLUSIONS

In summary, two dicarboxylate-substituted titanium-oxo-clusters, Ti₆O₄(*o*-BDC)₂(*o*-BDC-*i*Pr)₂(*O*^{*i*}Pr)₁₀ (**1**) and Ti₆O₃(*o*-BDC)₂(*O*^{*i*}Pr)₁₄ (**2**), have been prepared successfully via a one-step in situ solvothermal synthesis. They are the first examples of dicarboxylate-substituted oxo-alkoxy titanium clusters that the structures are measured by single-crystal X-ray analysis. The two Ti₆ clusters of **1** and **2** are constructed by two dual corner-missing cube subunit, Ti₃O₃, linked by μ₃-O and μ₂-O bridges, respectively. The skeletal arrangement of **2**

is a new type of Ti₆ carboxylate-substituted oxo clusters that has only a mono μ₂-O center bridge. Moreover, the crystals show a photochromic behavior in the presence of alcohol, and Ti(III) signal can be detected after irradiation. In the presence of oxygen, titanium(III) reduces molecular oxygen to superoxide diatomic O₂^{•-} radical. The photodegradation of the Methyl Orange (MO) in aqueous dispersions of microcrystals of the clusters was carried out under UV cut white light in the presence of tiny amount of H₂O₂. More than 90% decay of MO was observed over a period of 100 min. These well-characterized new clusters are the promised compounds in photocatalysis and solar harvesting.

ASSOCIATED CONTENT

Supporting Information

Crystallographic data of **1** and **2** in CIF format have been deposited with *Inorganic Chemistry*. These materials, and figures showing the XRD, IR ESR, and TGA analyses are available free of charge via the Internet at <http://pubs.acs.org>.

AUTHOR INFORMATION

Corresponding Author

*E-mails: zhuqinyu@suda.edu.cn (Q.Y.Z.); daijie@suda.edu.cn (J.D.).

Notes

The authors declare no competing financial interest.

ACKNOWLEDGMENTS

We gratefully acknowledge financial support by the NSF of China (No. 20971092), the Education Committee of Jiangsu Province (No. 11KJA150001), the Priority Academic Program Development of Jiangsu Higher Education Institutions, and the Program of Innovative Research Team of Soochow University.

REFERENCES

- (1) (a) Chen, X.; Mao, S. S. *Chem. Rev.* **2007**, *107*, 2891–2959. (b) Thompson, T. L.; Yates, J. T. *Chem. Rev.* **2006**, *106*, 4428–4453. (c) Chen, C.; Ma, W.; Zhao, J. *Chem. Soc. Rev.* **2010**, *39*, 4206–4219. (d) Liu, G.; Wang, L.; Yang, H. G.; Cheng, H.-M.; Lu, G. Q. *J. Mater. Chem.* **2010**, *20*, 831–843. (e) Gratzel, M. *Acc. Chem. Res.* **2009**, *42*, 1788–1798. (f) Yan, J.; Zhou, F. *J. Mater. Chem.* **2011**, *21*, 9406–9418.
- (2) (a) Benedict, J. B.; Coppens, P. *J. Am. Chem. Soc.* **2010**, *132*, 2938–2944. (b) Corden, J. P.; Errington, W.; Moore, P.; Partridge, M. G.; Wallbridge, M. G. H. *Dalton Trans.* **2004**, 1846–1851. (c) Steunou, N.; Kickelbick, G.; Boubekour, K.; Sanchez, C. *J. Chem. Soc., Dalton Trans.* **1999**, 3653–3655. (d) Campana, C. F.; Chen, Y.; Day, V. W.; Klemperer, W. G.; Sparks, R. A. *J. Chem. Soc., Dalton Trans.* **1996**, 691–702. (e) Day, V. W.; Eberspacher, T. A.; Klemperer, W. G.; Park, C. W. *J. Am. Chem. Soc.* **1993**, *115*, 8469–8410.
- (3) Benedict, J. B.; Freindorf, R.; Trzop, E.; Cogswell, J.; Coppens, P. *J. Am. Chem. Soc.* **2010**, *132*, 13669–13671.
- (4) Rozes, L.; Sanchez, C. *Chem. Soc. Rev.* **2011**, *40*, 1006–1030.
- (5) Pandey, A.; Gupta, V. D.; Noth, H. *Eur. J. Inorg. Chem.* **2000**, 1351–1357.
- (6) Dan-Hardi, M.; Serre, C.; Frot, T.; Rozes, L.; Maurin, G.; Sanchez, C.; Ferey, G. *J. Am. Chem. Soc.* **2009**, *131*, 10857–10859.
- (7) (a) Pflugrath, J. W. *Acta Crystallogr., Sect. D: Biol. Crystallogr.* **1999**, *55*, 1718–1725. (b) Rigaku Corporation, 1999. (c) CrystalClear Software User's Guide; Molecular Structure Corporation, 2000.
- (8) (a) Sheldrick, G. M. *Acta Crystallogr., Sect. A: Found. Crystallogr.* **2008**, *64*, 112–122. (b) Sheldrick, G. M. SHELXS-97, Program for structure solution; Universität of Göttingen, Göttingen, Germany, 1999. (c) Sheldrick, G. M. SHELXL-97, Program for structure refinement, Universität of Göttingen, Göttingen, Germany, 1997.

(9) Eslava, S.; McPartlin, M.; Thomson, R. I.; Rawson, J. M.; Wright, D. S. *Inorg. Chem.* **2010**, *49*, 11532–11540.

(10) (a) Boyle, T. J.; Tyner, R. P.; Alam, T. M.; Scott, B. L.; Ziller, J. W.; Potter, B. G. *J. Am. Chem. Soc.* **1999**, *121*, 12104–12112. (b) Ammala, P. S.; Batten, S. R.; Kepert, C. M.; Spiccia, L.; Van den Bergen, A. M.; West, B. O. *Inorg. Chim. Acta* **2003**, *353*, 75–81. (c) Boyle, T. J.; Alam, T. M.; Tafoya, C. J.; Scott, B. L. *Inorg. Chem.* **1998**, *37*, 5588–5594. (d) Papiernik, R.; Hubert-Pfalzgraf, L. G.; Vaisermann, J.; Goncalves, M. J. *Chem. Soc., Dalton Trans.* **1998**, 2285–2287. (e) Piszczek, P.; Grodzicki, A.; Richert, M.; Wojtczak, A. *Inorg. Chim. Acta* **2004**, *357*, 2769–2775. (f) Piszczek, P.; Richert, M.; Wojtczak, A. *Polyhedron* **2008**, *27*, 602–608.

(11) (a) Moraru, B.; Husing, N.; Kickelbick, G.; Schubert, U.; Fratzl, P.; Peterlik, H. *Chem. Mater.* **2002**, *14*, 2732–2740. (b) Lei, X. J.; Shang, M. Y.; Fehlner, T. P. *Organometallics* **1997**, *16*, 5289–5301. (c) Lei, X. J.; Shang, M. Y.; Fehlner, T. P. *Organometallics* **1996**, *15*, 3779–3781. (d) Ammala, P. S.; Batten, S. R.; Kepert, C. M.; Spiccia, L.; Bergen, A. M.; West, B. O. *Inorg. Chim. Acta* **2003**, *353*, 75–81. (e) Heinz, P.; Puchberger, M.; Bendova, M.; Baumann, S. O.; Schubert, U. *Dalton Trans.* **2010**, *39*, 7640–7644. (f) Gao, Y.; Kogler, F. R.; Peterlik, H.; Schubert, U. J. *Mater. Chem.* **2006**, *16*, 3268–3276. (g) Laaziz, P. I.; Larbot, A.; Guizard, C.; Durand, J.; Cot, L.; Joffre, J. *Acta Crystallogr., Sect. C: Cryst. Struct. Commun.* **1990**, *46*, 2332–2334. (h) Kickelbick, G.; Holzinger, D.; Brick, C.; Trimme, G.; Moons, E. *Chem. Mater.* **2002**, *14*, 4382–4389. (i) Mijatovic, I.; Kickelbick, G.; Schubert, U. *Eur. J. Inorg. Chem.* **2001**, 1933–1935.

(12) (a) Fisher, M. F. *Am. J. Phys.* **1964**, *32*, 343–346. (b) Wendlandt, W. W.; Hecht, H. G. *Reflectance Spectroscopy*; Interscience Publishers: New York, 1966.

(13) (a) Prakash, A. M.; Kurshev, V.; Kevan, L. J. *Phys. Chem. B* **1997**, *101*, 9794–9799. (b) Murata, C.; Yoshida, H.; Kumagai, J.; Hattori, T. *J. Phys. Chem. B* **2003**, *107*, 4364–4373.

(14) (a) Yu, L.; Xi, J.; Li, M.-D.; Chan, H. T.; Su, T.; Phillips, D. L.; Chan, W. K. *Phys. Chem. Chem. Phys.* **2012**, *14*, 3589–3595. (b) Yang, J.; Chen, C.; Ji, H.; Ma, W.; Zhao, J. *J. Phys. Chem. B* **2005**, *109*, 21900–21907. (c) Chen, C.; Li, X.; Ma, W.; Zhao, J. *J. Phys. Chem. B* **2002**, *106*, 318–324.

(15) (a) Rao, Y. F.; Chu, W. *Environ. Sci. Technol.* **2009**, *43*, 6183–6189. (b) Wang, C. C.; Chu, W. *Environ. Sci. Technol.* **2003**, *37*, 2310–2316. (c) Hirakawa, T.; Nosaka, Y. *Langmuir* **2002**, *18*, 3247–3254. (d) Selvin, R.; Hsu, H.; Arul, N. S.; Mathew, S. *Sci. Adv. Mater.* **2010**, *2*, 58–63.

(16) Zhao, J.; Wu, T.; Wu, K.; Oikawa, K.; Hidaka, H.; Serpone, N. *Environ. Sci. Technol.* **1998**, *32*, 2394–2400.